

Article

Energy-Economizing Optimization of Magnesium Alloy Hot Stamping Process

Mengdi Gao ¹, Qingyang Wang ^{1,*}, Lei Li ² and Zhilin Ma ¹

¹ School of Mechanical and Electronic Engineering, Suzhou University, Suzhou 234000, China; gaomengdi@ahszu.edu.cn (M.G.); mazhilin018@163.com (Z.M.)

² School of Mechanical Engineering, Hefei University of Technology, Hefei 230000, China; lei_li@hfut.edu.cn

* Correspondence: wangqingyang@ahszu.edu.cn; Tel.: +86-1780-557-5586

Received: 24 December 2019; Accepted: 23 January 2020; Published: 5 February 2020



Abstract: Reducing the mass of vehicles is an effective way to improve energy efficiency and mileage. Therefore, hot stamping is developed to manufacture lightweight materials used for vehicle production, such as magnesium and aluminum alloys. However, in comparison with traditional cold stamping, hot stamping is a high-energy-consumption process, because it requires heating sheet materials to a certain temperature before forming. Moreover, the process parameters of hot stamping considerably influence the product forming quality and energy consumption. In this work, the energy-economizing indices of hot stamping are established with multiobjective consideration of energy consumption and product forming quality to find a pathway by which to obtain optimal hot stamping process parameters. An energy consumption index is quantified by the developed models, and forming quality indices are calculated using a finite element model. Response surface models between the process parameters and energy-economizing indices are established by combining the Latin hypercube design and response surface methodology. The multiobjective problem is solved using a multiobjective genetic algorithm (NSGA-II) to obtain the Pareto frontier. ZK60 magnesium alloy hot stamping is applied as a case study to obtain an optimal combination of parameters, and compromise solutions are compared through stamping trials and numerical simulations. The obtained results may be used for guiding process optimization regarding energy saving and the method of manufacturing parameters selection.

Keywords: energy-economizing; hot stamping; lightweight material; magnesium alloy; process parameters

1. Introduction

Rapid economic development has recently accelerated increases in the consumption of energy, especially in industrial sectors, which is causing a series of environmental problems, such as greenhouse gas (GHG) emissions [1]. The GHG emissions in China reach 1.03×10^9 T, of which 10–15% come from automobiles [2]. An efficient way to improve the energy efficiency and driving range of vehicles is mass reduction. Some lightweight materials, such as magnesium alloys, aluminum alloys, and ultra-high-strength steels, have been rapidly increasing in quantity and have been applied to the automotive industry [3]. Vehicles can conserve significant amounts of energy by using these lightweight materials [4].

Hot stamping was developed to manufacture the structural components of automobiles by using lightweight materials to achieve decreased weight, improved safety, and enhanced crashworthiness [5]. Hot stamping can improve the formability of these lightweight materials, which overcomes the limits of traditional cold stamping [6]; it is particularly suitable for manufacturing complex parts [7]. Moreover,

the high forming precision and reduced springback of hot stamping have led to its wide application in the automotive and aircraft industries.

However, the high-temperature forming conditions of blanks in the hot stamping process consume additional energy. Heating the sheet material to a certain temperature improves the energy consumption of hot stamping compared with that of cold stamping [8]. The energy consumption and environmental effects of the hot stamping industry warrant attention. Process energy consumption models of hot stamping have been developed to qualify its energy consumption [9]. The associated carbon footprint is identified to analyze its environmental effects [10]. All the results show that oven curing accounts for a large amount of the products' energy consumption and environmental impact. Therefore, one efficient pathway towards energy-economizing hot stamping is promoting the energy efficiency in the blank heating process. The thermal transfer and loss principle is basic for energy efficiency improvement in oven curing. To study the thermal aspects of the hot stamping process, based on the identification of the heat transfer coefficient in hot stamping [11], Abdulhay et al. proposed the heat-transfer modeling of all heat-transfer modes occurring during the hot stamping phases [12].

A suitable stamping temperature is very important in optimizing the energy efficiency of hot stamping. The product forming quality and energy consumption are determined by process parameters. Many researchers have focused on the optimization of these parameters to solve the product forming quality problem of hot stamping. Xiao et al. found that decreasing forming temperature and increasing forming speed can improve the formability of AA7075 through a hot uniaxial tensile test [13]. More than one object should be considered in multiobjective optimization methods, such as the weighted sum method [14], the global criterion-based method [15], and genetic algorithms [16], which are widely applied in the hot stamping to solve the conflict between different evaluation indices of forming quality. Kitayama et al. used sequential approximate optimization with radial basis function network to optimize the parameter of blank holder force trajectory, with the aim of reducing the products' springback [17]. Zhou et al. focused on numerical simulations, together with the combination of response surface methodology (RSM) and nondominated sorting genetic algorithm II (NSGA-II) to optimize aluminum alloy hot stamping [18]. In order to reduce the influence of the stochastic property of process parameters on forming quality, Xiao et al. integrated multiobjective stochastic approaches, such as RSM, NSGA-II, and Monte Carlo simulations (MCSs), to obtain the optimal process parameters of aluminum hot stamping [19].

The above analysis reveals that the energy consumption and environmental soundness of the hot stamping process are of serious concern. But research on how to reduce the energy consumption of the hot stamping process is still insufficient. Process optimization is an excellent way to solve this problem. But the process parameters have been optimized using numerous methods and multiobjective optimization methods to enhance only the product forming quality. Energy consumption should not be neglected in the parameters optimization of the hot stamping process. In particular, hot stamping optimization with consideration for energy saving is worth studying due to its relevance to energy-efficient manufacturing. However, there is still a lack of effective methods regarding both the optimization of energy consumption and in terms of improving the forming quality at present. In this study, a novel parameter optimization method for the hot stamping process is proposed with the multiobjective improvement of forming quality and process energy consumption.

2. Framework and Method

Different process parameters determine the amount of energy consumption and product forming quality of hot stamping. Product forming defects, such as wrinkles, cracks, or high energy consumption, will appear when sheet materials are processed under inappropriate process parameters. This can be avoided by adjusting and selecting appropriate process parameters in hot stamping. Process optimization is an efficient way to reduce the energy consumption and avoid forming defects in the hot stamping process.

A descriptive flowchart depicting the major steps of the proposed methodology is shown in Figure 1, which provides an outline for this study. A hot stamping process contains heating and forming processes; energy and material are supplied for the process with different processing parameters. In order to achieve an environmentally-friendly manufacturing process, energy reduction is essential. Process energy consumption and forming quality are considered in the process optimization method of hot stamping, which are taken as the energy-economizing indices. These indices of hot stamping are regarded as the optimization objectives. The forming quality and energy consumption under different process parameters are qualified by the developed models or simulation and experiments. The range and constraints of the optimized process parameters should be initially determined in accordance with the forming performance and requirements. Then, sample points should be selected in the design space for experiments, and the corresponding simulations or experiments be conducted to obtain the corresponding evaluation index values of each sample point. Our model was developed to study the relationship between the process parameters and each index, which was solved using a multiobjective genetic algorithm (NSGA-II) and offers feasible optimized solutions. The comparison between the numerically-predicted technical parameters of the stamps and the real experimental results demonstrate the applicability of the method. The multiobjective optimization method can improve the energy efficiency of hot stamping while maintaining the required quality of the stamps. The proposed energy-economizing can provide a reference for industrial manufacturing and production, especially for vehicle production.

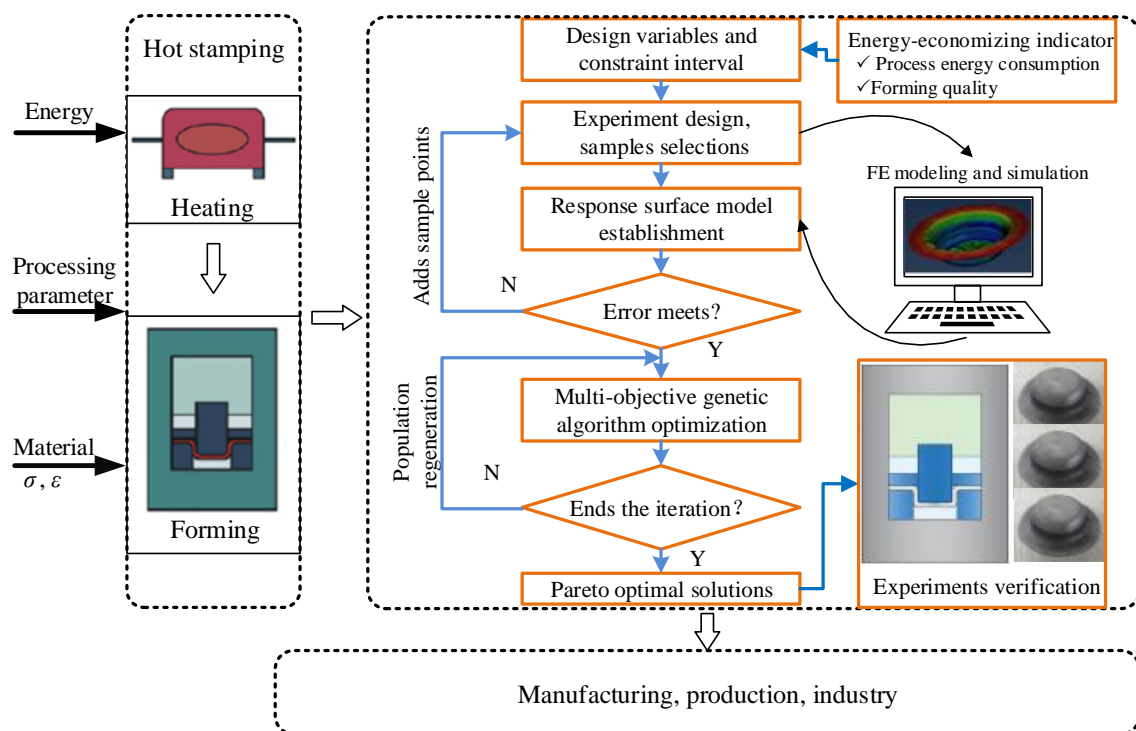


Figure 1. Methodological framework.

3. Energy-Economizing Indices of Hot Stamping

3.1. Process Energy Consumption Indices

The hot stamping process begins by heating a sheet material to a given range of temperatures to improve formability. Therefore, the energy consumption of hot stamping is associated with the energy

used for heating and that used for forming. The total energy consumption of hot stamping, E , can be calculated as

$$E = E_{\text{heating}} + E_{\text{forming}}, \quad (1)$$

where E_{heating} is the heating energy consumption and E_{forming} is the forming energy consumption.

After being heated in a furnace, the sheet material is delivered to a piece of forming equipment and immediately formed in a closed tool. Thus, the heat is transferred to the environment and tools in those processes; this transfer is described as heat loss, ΔQ . The heat loss includes convection and radiation losses with ambient air during the transfer to the forming equipment, and the losses by heterogeneous approaches of convection, radiation, and conduction in the forming process [12]. Therefore, the heat loss (ΔQ) can be calculated as

$$\Delta Q = Q_{\text{convection}} + Q_{\text{radiation}} + Q_{\text{conduction}}, \quad (2)$$

where $Q_{\text{convection}}$, $Q_{\text{radiation}}$, and $Q_{\text{conduction}}$ are the heat losses by convection, radiation, and conduction, respectively, and can be calculated by as follows:

$$Q_{\text{convection}} = Q(R_h, \Delta T, \Delta t) = Ah\Delta T\Delta t, \quad (3)$$

$$Q_{\text{radiation}} = kF_r A((T + \Delta T)^4 - T^4)\Delta t, \quad (4)$$

$$Q_{\text{conduction}} = Q(R_\lambda, \Delta T, \Delta t) = A\lambda \frac{\Delta T}{t_0} \Delta t, \quad (5)$$

where A is the heat transfer area, h is the convection coefficient, $R_h = 1/Ah$ is the convection resistance, T is the temperature, ΔT is the temperature difference between hot and cold fluid object, k is the Boltzmann constant, F_r is the radiation shape factor, λ is the thermal conductivity, and $R_\lambda = \delta/A\lambda$ is the thermal resistance, δ is the thickness, t is the time.

The total heat, Q , can be calculated by Equation (6), which combines the heat in the blank and the heat loss.

$$Q = Q_{\text{blank}} + \Delta Q, \quad (6)$$

where Q_{blank} is the heat absorbed by sheet metal.

The energy consumption used for heating can be calculated as

$$E_{\text{heating}} = \frac{Q}{1 - \eta_{\text{loss}}(T, i)}, \quad (7)$$

where $\eta_{\text{loss}}(T, i)$ is thermal efficiency loss caused by the different heating temperatures and methods and i denotes the three heating means, namely, radiation, induction, and conduction.

The forming stage in hot stamping is similar to that in cold stamping, as shown in Figure 2. The heated sheet material is placed on a die with a blank holder to avoid wrinkle defects. The forming press controls the punch to draw the blank into the die and to form it into the desired shape with the elastic–plastic deformation of the sheet metal and the contact friction between the sheet material and dies [20]. Therefore, the energy consumption of the forming stage in the hot stamping process can be quantified from two perspectives. The direct ways are measuring and estimating the energy consumption of the forming equipment [21], which can be described as

$$E_{\text{forming}} = \int_{t_{\text{start}}}^{t_{\text{end}}} F(t)v(t)dt/\eta(t), \quad (8)$$

where F is the output force of the actuator of the forming equipment, which varies with the working conditions; v is the punch speed, and η is the energy efficiency in the stamping process.

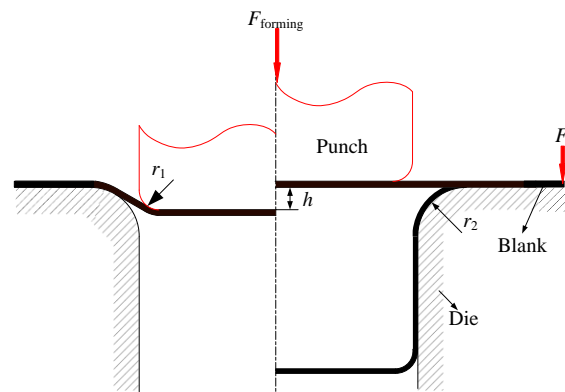


Figure 2. Forming process of hot stamping.

The second method involves consideration of the deformation process of the sheet material, and then analysis and modeling of the process energy consumption with the related parameters. The energy consumption of the sheet metal forming process may be divided into that required for plastic deformation, bending, and frictional energies [8]. These analytical quantification methods of calculating the process energy consumption are detailed in Reference [22].

3.2. Forming Quality Indices

The thinning and thickening of critical elements are used to indicate whether fractures have occurred in the blank forming process. Springback cannot be regarded as a forming quality index because the springback of hot stamping is considerably less than that of cold stamping. A sheet metal will crack if its thickness is less than a certain critical value. The rupture distance refers to the vertical distance between the strain point of dangerous elements and the forming limit curve (FLC), as shown in Figure 3. When the main strain of a region element of the formed part is above the FLC ($\varphi(\varepsilon_2)$) or the safety marginal curve ($\Phi(\varepsilon_2)$), this region of the shaped part will likely fracture. A long distance from the safety marginal curve $\Phi(\varepsilon_2)$ indicates a high rupture tendency. Therefore, the average distance between the main strain of all elements and the $\Phi(\varepsilon_2)$ curve can be used to quantify the fracture. Similarly, when the main strain of an area element is below the wrinkle limit curve ($\psi(\varepsilon_2)$), this area of the formed part will show a wrinkling trend; the farther the point from the $\psi(\varepsilon_2)$ curve, the higher the trend of wrinkling. The fracture distance and wrinkling trend are mainly used to predict the product forming quality in the finite element (FE) simulation, but the FLC limit diagram cannot be directly used to quantify the product forming quality in the actual stamping production process.

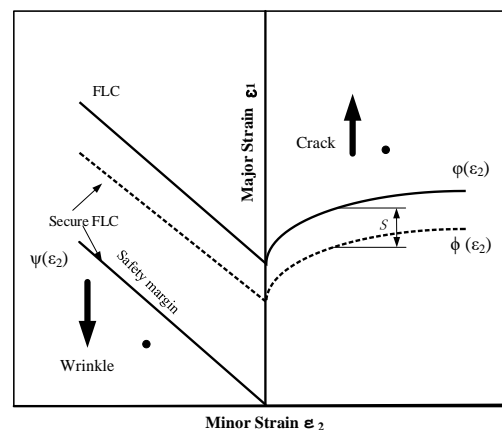


Figure 3. Definition diagram of cracking and wrinkling quantification criteria. $\Phi(\varepsilon_2)$ is the safety marginal curve, $\psi(\varepsilon_2)$ is the wrinkle limit curve, and $\varphi(\varepsilon_2)$ is the FLC.

Therefore, in the actual production and the experiment, thinning and thickening can be used to represent the possibility of fracture and wrinkling, respectively. These indices are calculated using Equations (9) and (10). An excessively large thinning rate of a sheet metal in a certain area means that the fracture trend is too large, whereas a disproportionately high thickening rate indicates a possible wrinkling phenomenon.

$$\Delta_{\text{thinning}} = (t_0 - t_{\min}) / t_0 \times 100\%, \quad (9)$$

$$\Delta_{\text{thickening}} = (t_{\max} - t_0) / t_0 \times 100\%, \quad (10)$$

where t_0 is the thickness of the blank, t_{\min} is the minimum thickness of the sheet material, t_{\max} is the maximum thickness of the sheet material, Δ_{thinning} is the thinning rate, and $\Delta_{\text{thickening}}$ is the thickening rate.

4. Multiobjective Optimization for Hot Stamping Process

4.1. Optimization Variables

The considered process parameters are regarded as optimization variables in the hot stamping optimization process. Many process parameters affect the energy consumption and forming quality of stamping parts, such as stamping speed, blank holder force, friction conditions, tool gap, and draw-bead geometry parameters. The influence of the draw-bead is usually not considered because the draw-bead is typically used only in stamping extremely complex-shaped parts. In addition, the shape parameters of the draw-bead are complex, and have independent design criteria for some simple stamping processes. The clearance between the punch and die substantially affects the springback of the forming parts, which usually accounts for 110–120% of the sheet metal thickness. The die gap is usually ignored as a design variable because of the small springback in the hot stamping process. No quantitative analysis exists for the effect of friction on product forming quality because the friction conditions in an actual stamping workshop are determined by the lubricating oil, die material, and coating. Therefore, in hot stamping optimization, three process parameters, namely, stamping speed, blank holder force, and forming temperature, should be considered. A certain range of process parameters should be experimentally analyzed to obtain the optimal process parameters.

After the optimization variables are determined, a certain sample point is selected in the design space for experiment. The surrogate model between each process parameter and its corresponding index value is established on the basis of RSM, and the process parameters are optimized on the basis of the multiobjective genetic algorithm.

4.2. Sample Selection

The Latin hypercube design (LHD) is an efficient sampling method; it is advantageous in sampling efficiency and running time due to its reduced number of iterations. This method is especially suitable for computer simulation experiments. A good feature of this method is that sample points are selected from the entire design space. Therefore, the optimal process parameters can be determined systematically and accurately with less experiments by using this method. LHD evenly divides the design space of each variable into several layers, and these layers obtain some special points through random combination to determine the design matrix. Each level of each parameter is sampled only once.

4.3. Optimization Model and Solution Approach

The energy-economizing optimization aims to obtain a set of process parameters that will produce stamping parts with good forming quality (no cracks, wrinkling, or noticeable thickening and thinning)

and low energy consumption. The objective function and constraints of the optimization process can be given as

$$\begin{aligned} F &= \min(y_1, y_2, y_3) \\ \text{s.t.} \quad &\begin{cases} h_i(x) = 0 \quad (i = 1, 2 \dots n) \\ g_j(x) \geq 0 \quad (j = 1, 2 \dots n) \\ x_m^{\min} < x_m < x_m^{\max} \quad (m = 1, 2 \dots n) \end{cases} \end{aligned} \quad (11)$$

where y_1 , y_2 , and y_3 are the response functions of the energy-economizing indices, namely, energy consumption, thinning, and thickening, respectively, and x_m are the design variables, namely, blank holder force, stamping speed, and forming temperature.

Determining the mapping function through theoretical derivation is difficult due to the complex relationship between process parameters and target quantity. RSM is an effective method of building substitute models. The RSM polynomial regression model adopts a quadratic regression equation. On the basis of experimental data, the coefficient of the regression equation is obtained through the least squares method to construct the functional relationship between the optimization variable and target quantity. The commonly used second-order polynomial response surface model can be represented by

$$y = a_0 + \sum_{i=1}^n a_i x_i + \sum_{i=1}^n a_{ii} x_i^2 + \sum_{i=2}^n \sum_{j=1}^{i-1} a_{ij} x_i x_j, \quad (12)$$

where x_i , x_j represents the design variable; n is the minimum number of samples; a_0 is the minor error; a_i , a_{ii} , and a_{ij} are the polynomial coefficients; and y represents the response of the energy-economizing indices of the stamping process.

NSGA-II is a multiobjective genetic algorithm that ensures good convergence and robustness by introducing a fast nondominated sorting algorithm, elite strategy, and congestion degree comparison operator, and other strategies [23]. The multiobjective optimization problem of hot stamping can be solved by programming NSGA-II.

5. Hot Stamping Process Optimization of ZK60 Magnesium Alloy for Energy Saving

On the basis of the proposed energy-economizing optimization method of hot stamping, the tube-shaped part, whose common profile is shown in Figure 4, is selected as a case to investigate the proposed method. Table 1 presents the tool size and relevant parameters of the sheet metal. The stamping material is ZK60 magnesium alloy, which is a lightweight material with strong deformation capability and good heat treatment strengthening effect. Three variable process parameters, namely, stamping speed (v), blank holder force (F_h), and forming temperature (T), are considered in the simulation process. The range of each process parameter is set as follows: stamping speed 2–11 mm/s, blank holder force 3–9 kN, and forming temperature 175–250 °C (the range of forming temperature is determined on the basis of existing research results in Reference [24]).

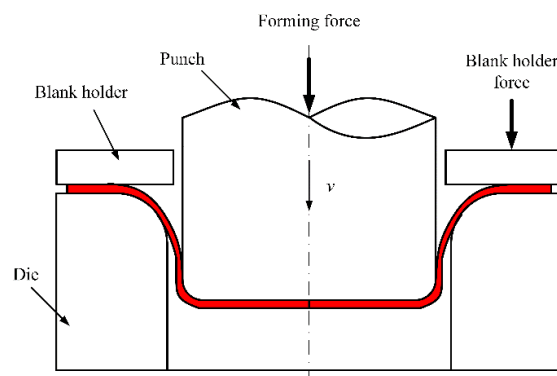
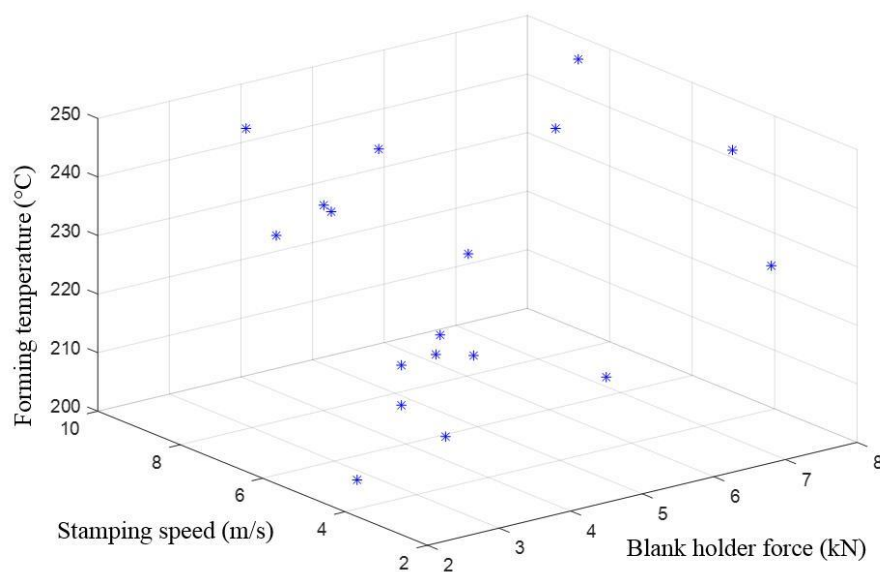


Figure 4. Stamping of tube-shaped part.

Table 1. Parameters for drawing processes of tube-shaped parts.

| Blank Diameter d_p (mm) | Sheet Metal Thickness t_0 (mm) | Drawing Height h (mm) | Punch Radius r_1 (mm) | Die Radius r_2 (mm) | Clearance δ (mm) | Friction Coefficient μ |
|------------------------------|-------------------------------------|----------------------------|----------------------------|--------------------------|----------------------------|-------------------------------|
| 100.0 | 1.0 | 20.0 | 7.0 | 8.0 | 1.2 | 0.12 |

On the basis of the aforementioned experimental design method, the LHD sampling method is used to sample the point in the range of each process parameter, and the least number of sample points required by the response surface model is determined through the least squares method. The number of samples n can be determined in terms of the equation $n = (m + 1)(m + 2)/2$ of the number of considered process parameters m . Given that the number of process parameters m is 3, the number of samples n is at least 10. Eighteen design sample points are selected to improve the accuracy of the response surface model, and Figure 5 illustrates their value distribution.

**Figure 5.** Sample distribution of LHD in the range of each process parameter.

5.1. Material Properties Testing

Accurate mechanical property parameters and an equivalent stress model are vital for analyzing the hot deformation of magnesium alloy. The goal is to identify the mechanical properties of ZK60 magnesium alloy under different temperatures, which are used for the theoretical calculation of energy consumption and simulation. Table 2 shows the chemical composition of ZK60 magnesium alloy. A series of hot unidirectional tensile experiments is performed on an MTS810 system material testing machine (Figure 6) at different temperatures. The testing samples are designed on the basis of the GB/T4338-2006 high-temperature tensile testing method of metallic materials, and the thickness of the samples is 2 mm, as shown in Figure 7.

Table 2. ZK60 magnesium alloy chemical composition (%).

| Element | Si | Fe | Cu | Mn | Al | Zn | Ni | Zr |
|-------------------|--------|-------|--------|-------|--------|-----|---------|------|
| Quality score w | 0.0014 | 0.003 | 0.0011 | 0.008 | 0.0014 | 5.5 | 0.00048 | 0.53 |

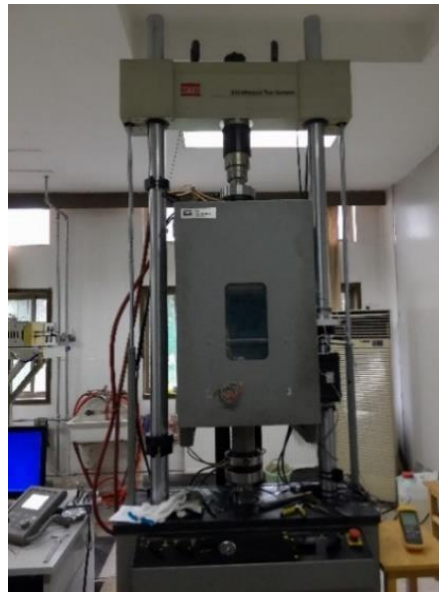


Figure 6. MTS810 material experimental system.

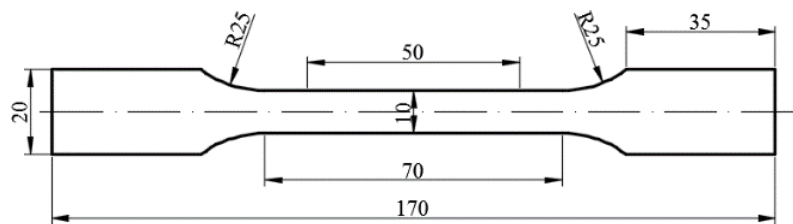


Figure 7. ZK60 magnesium alloy tensile sample.

The hot unidirectional tensile experiments are performed under invariable temperatures of 175 °C, 200 °C, 225 °C, and 250 °C. The samples are kept in an environmental cabinet for 15 min after being clamped at different temperatures. The samples are then stretched with different speeds to obtain the stress-strain curve of ZK60. Three groups of experiments are conducted under the same parameters, and the average values are regarded as the experimental results under the corresponding conditions. Figure 8 exhibits the obtained true stress–strain curve of ZK60 magnesium alloy.

A flow stress mathematical model of ZK60 magnesium alloy is established on the basis of the Fields–Backofen equation in consideration of the softening factor proposed by Zhang et al. [25]. In accordance with the experimental stress–strain curves of ZK60 magnesium alloy under various temperatures, the corresponding flow stress mathematical model is developed as

$$\sigma = 746\varepsilon^{0.1101}\dot{\varepsilon}^{0.0262}\exp(-0.00665T - 0.94781\varepsilon), \quad (13)$$

where σ is the stress of the investigated ZK60 magnesium alloy, ε is the strain of the ZK60 magnesium alloy, and $\dot{\varepsilon}$ is the strain rate of ZK60 magnesium alloy.

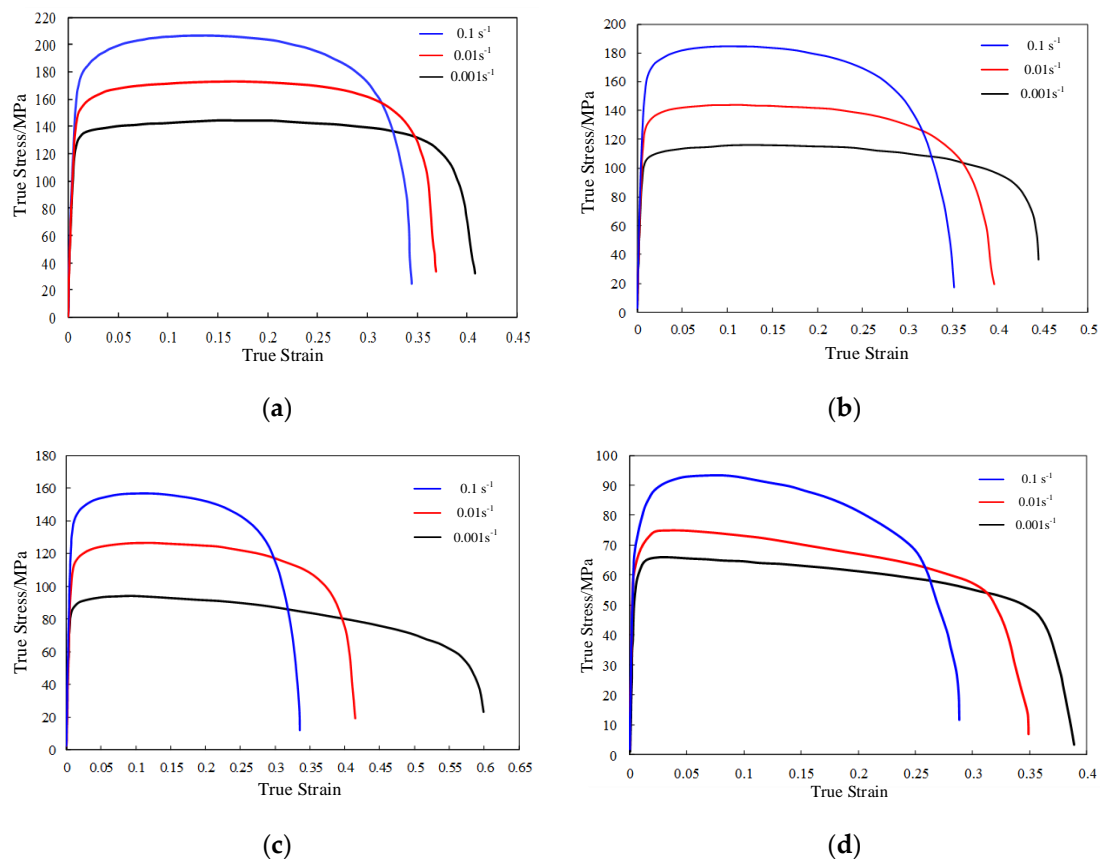


Figure 8. True stress-strain curves for ZK60 magnesium alloy deformed at different temperatures and strain rates: (a) 175 °C; (b) 200 °C; (c) 225 °C; (d) 250 °C.

5.2. FE Modeling and Simulation for Hot Stamping

The FE simulation model is established in accordance with the actual hot stamping process, as shown in Figure 9. The punch is placed above the sheet metal, the die is at the bottom, and the sheet metal lies above the die and below the blank holder. In the simulation process, the mold is regarded as a rigid body without elastic deformation; thus, it cannot be meshed. A Belytschko–Tsay shell element with five Gaussian thickness dimension integration points is used to divide the sheet metal mesh, and the thickness of the sheet metal is set as 1 mm. The initial unit number of the sheet metal is 3925, and the grid refinement level is set as 2. The kinematic relations of the tools and blank are as follows:

- (1) Figure 9 depicts the initial positions of the die and blank, and the sheet metal is above the die.
- (2) The blank holder is close to the sheet metal at a certain speed (it can be set to different speeds, but it maintains a constant speed throughout the stamping process), which is called “holding.”
- (3) When the blank holder is finished, the sheet metal is fixed, and the punch starts to act. The “stamping” process begins when the punch contacts the sheet metal.
- (4) In the last stage of the simulation, the concave convex die is in a closed state, followed by the quenching stage.

In accordance with the friction condition between the blank and tools in the actual stamping process, the friction coefficient is set as 0.12 in the simulation. The blank is heated via in-mold heating. This heating method is advantageous in that the variation of temperature is relatively small; therefore, the temperature distribution of the sheet is uniform and has good formability. However, the energy consumption used for heating will be considerably higher than that for furnace heating. The simulations are performed on the basis of the design points in Figure 5, and the corresponding

energy consumption is calculated through a previous energy consumption theoretical model. Table 3 shows the results.

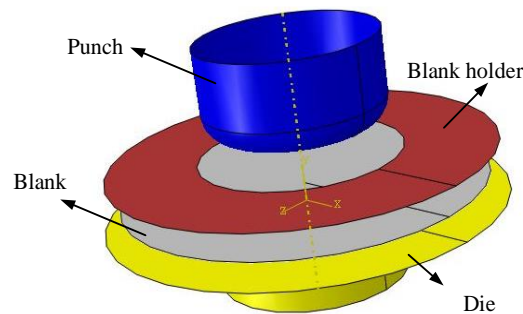


Figure 9. Numerical simulation model of the tube-shaped part.

Table 3. Experimental design points and corresponding results.

| Run | F_h (kN) | v (mm/s) | T (°C) | Energy Consumption (J) | Thinning (%) | Thickening (%) |
|-----|------------|------------|----------|------------------------|--------------|----------------|
| 1 | 2.1 | 4.7 | 250 | 46,212.27 | 5.09 | 8.1 |
| 2 | 2.5 | 3.5 | 225 | 32,165.84 | 4.3 | 8 |
| 3 | 2.8 | 5.1 | 200 | 28,919.08 | 4.32 | 7.3 |
| 4 | 3.1 | 8.3 | 250 | 48,726.87 | 5.96 | 7.6 |
| 5 | 3.5 | 4.3 | 225 | 33,066.23 | 9.62 | 6.8 |
| 6 | 3.8 | 6.3 | 250 | 47,463.92 | 5.78 | 7 |
| 7 | 4.2 | 9.5 | 225 | 37,347.17 | 9.64 | 7.8 |
| 8 | 4.5 | 5.9 | 200 | 29,853.32 | 7.71 | 6.8 |
| 9 | 4.8 | 7.5 | 200 | 31,439.71 | 5.08 | 7.4 |
| 10 | 5.2 | 9.9 | 225 | 37,667.46 | 7.75 | 8 |
| 11 | 5.5 | 7.1 | 225 | 35,622.90 | 7.01 | 7.1 |
| 12 | 5.8 | 5.5 | 250 | 46,978.99 | 16.12 | 6 |
| 13 | 6.2 | 9.1 | 200 | 32,932.06 | 6.12 | 7.7 |
| 14 | 6.5 | 8.7 | 200 | 32,596.56 | 6.04 | 7.5 |
| 15 | 6.9 | 3.1 | 250 | 44,981.23 | 6.74 | 6.2 |
| 16 | 7.2 | 6.7 | 200 | 30,775.07 | 5.84 | 7 |
| 17 | 7.5 | 7.9 | 250 | 48,664.86 | 8.59 | 6.4 |
| 18 | 7.9 | 3.9 | 225 | 32,835.24 | 11.86 | 5.7 |

5.3. Process Parameters Optimization

On the basis of the above results, a second-order regression model is used to obtain the response surface for each objective function. Let y_1 be the energy consumption of hot stamping, y_2 the thinning rate of the stamping parts, and y_3 the thickening rate of the stamping parts. The developed model can then be described as

$$y_1 = 261054 + 76.8495x_1 + 2643.08480x_2 - 2455.30317x_3 + 0.26751x_1x_2 - 0.17018x_1x_2 - 6.13451x_2x_3 + 0.14412x_1^2 - 31.95144x_2^2 + 6.31017x_3^2, \quad (14)$$

$$y_2 = -185.68990 - 0.037136x_1 + 0.58991x_2 + 1.68914x_3 - 0.16617x_1x_2 + 3.71659 \times 10^{-3}x_1x_3 + 4.68506 \times 10^{-3}x_2x_3 + 0.069271x_1^2 - 0.055531x_2^2 - 3.83894 \times 10^{-3}x_3^2, \quad (15)$$

$$y_3 = 0.78922 - 0.39606x_1 + 0.29588x_2 + 0.059743x_3 + 0.036733x_1x_2 - 2.74212 \times 10^{-3}x_1x_3 - 3.66213 \times 10^{-3}x_2x_3 + 0.050898x_1^2 + 0.041834x_2^2 - 6.34584 \times 10^{-5}x_3^2, \quad (16)$$

where x_1 is the blank holder force, x_2 is the stamping speed, and x_3 is the forming temperature.

Hot stamping process optimization aims to obtain a set of process parameters that will produce stamping parts with reduced thickness variations and low energy consumption. Therefore, the objective function and constraint conditions in the optimization process can be expressed as

$$F = \min(y_1, y_2, y_3)$$

$$s.t. \begin{cases} 2 \leq x_1 \leq 8 \\ 3 \leq x_2 \leq 10 \\ 200 \leq x_3 \leq 250 \end{cases}, \quad (17)$$

where y_1 , y_2 , and y_3 are the objective functions. The goal is to minimize the stamping energy consumption and thickness variations in hot stamping.

NSGA-II is used to solve the multiobjective optimization problem in Equation (17). A series of considered efficient solutions constituting the Pareto frontier is obtained, as shown in Figure 10. The results show that the formability and energy consumption of sheet metals are contradictory. For ZK60 magnesium alloy hot stamping, formability improves with the increase in forming temperature, but the energy consumption of hot stamping increases significantly with the rise of heating temperature. The thinning and thickening rates are also contradictory. With increasing blank holder force, the thinning rate of stamping parts increases gradually, whereas the wrinkling trend of the sheet metal decreases. On the basis of the forming requirements (the thinning and thickening rates of stamping must be less than 10%, and the energy consumption of stamping should be relatively small), the following two groups of compromise solutions are selected, and Table 4 presents the corresponding index values.

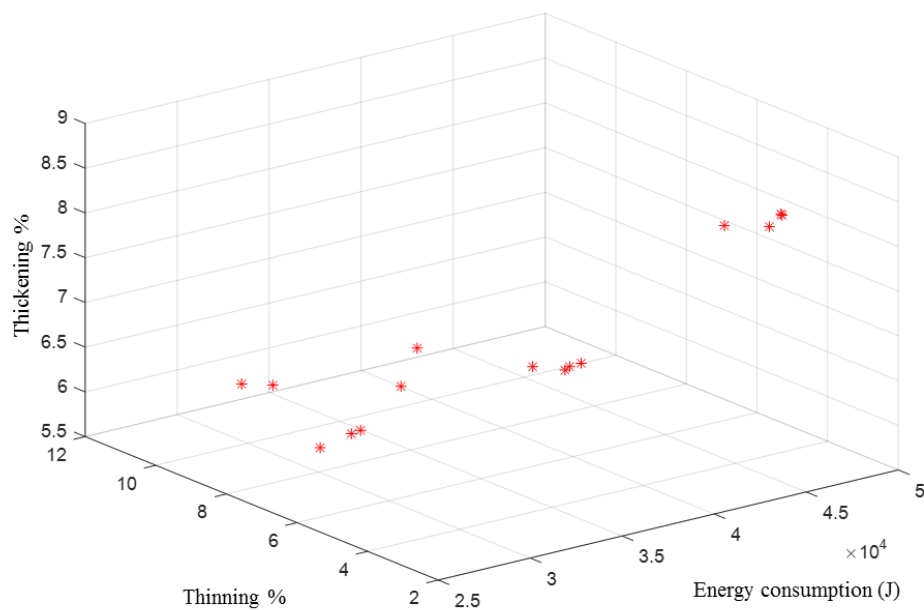


Figure 10. Pareto optimal solutions of ZK60 magnesium alloy hot stamping.

Table 4. Compromise solutions and their corresponding indices.

| Compromise Solutions | Process Parameters | | | Indices | | |
|----------------------|--------------------|------------|----------|------------------------|--------------|----------------|
| | F_h (kN) | v (mm/s) | T (°C) | Energy Consumption (J) | Thinning (%) | Thickening (%) |
| Solution 1 | 8.0 | 3.0 | 225 | 31,785.57 | 6.2 | 5.7 |
| Solution 2 | 4.7 | 3.3 | 200 | 26,190.36 | 4.8 | 5.9 |

Figure 11 shows the simulation results of the thickness variation distribution under different compromise solutions. The forming quality of stamping parts under the two groups of process parameters is good and can meet the usage requirements. The thicknesses of the stamping parts vary greatly in terms of punch and die radii. From the straight wall section to the flange area, from the bottom to the top, the thickness variation distribution of the parts presents a gradual increase trend at the parameters of the two compromise solutions, and the thickening phenomenon is shown in the flange area. A comparison of the color distribution of the thickness variation of the stamping parts in the simulation results indicates that the thickness variation distribution of the stamping parts obtained at the parameters of compromise solution 1 is slightly more uniform than that at the parameters of compromise solution 2. The energy consumption at the parameters of compromise solution 2 can be reduced by 17.6% in comparison with those in compromise solution 1. Therefore, considering all energy-economizing indices of hot stamping, the indices of energy consumption and thinning in compromise solution 2 are better than those in compromise solution 1.

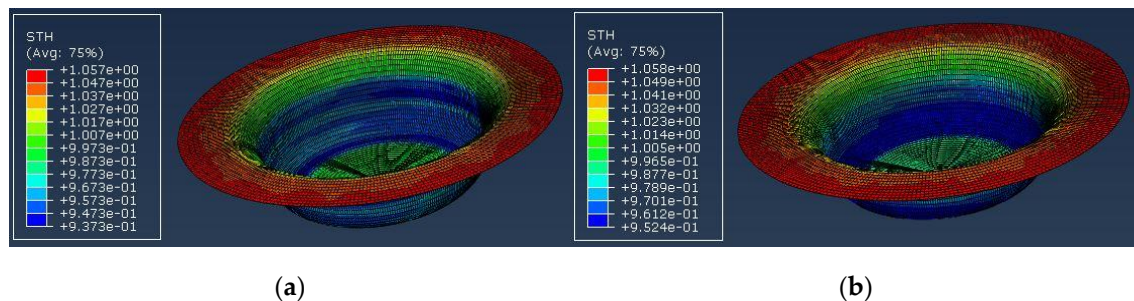


Figure 11. Thickness variation distribution demonstrated by the numerical simulation under different compromise solutions: (a) compromise solution 1, (b) compromise solution 2.

5.4. Stamping Experiments Verification

The corresponding experiment is conducted with experimental equipment to verify the feasibility of the optimization results for the hot stamping process, as shown in Figure 12. In accordance with the obtained compromise solutions, the experiments are performed as follows:

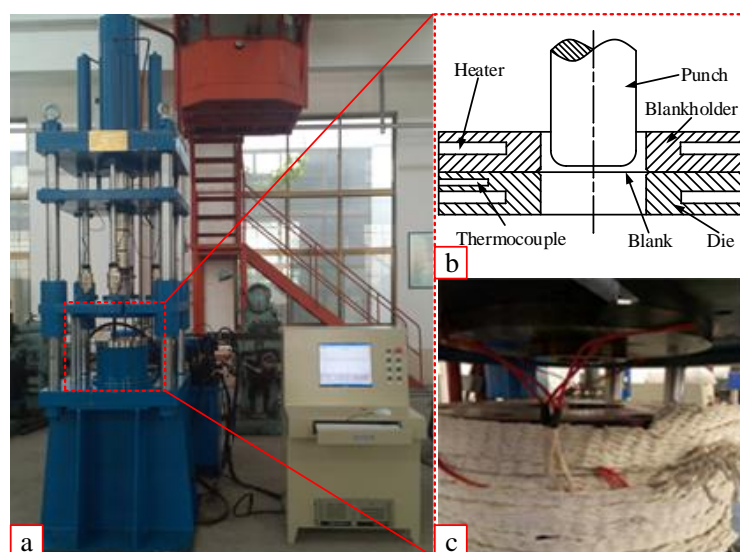


Figure 12. Equipment and die structures for hot stamping process of tube-shaped parts: (a) 100 T partitioned VBHF hydraulic machine, (b) die structure, (c) physical die.

The temperature in the die was raised to 225 °C by internal heating, as shown in Figure 12b,c. Then, the prepared ZK60 magnesium alloy sheet material is placed into the die, and the mold is closed. The heat preservation time is set as 10 min to heat the blank fully. The process parameters of the forming press are set as follows: 8 kN blank holder force and 3 mm/s stamping speed (Table 4). The stamping experiment is then conducted. Three groups of experiments are conducted in accordance with the above experimental steps. Then, to reduce the temperature of the die to 200 °C and repeat above experimental steps, the process parameters are set as follows: 4.7 kN blank holder force and 3.3 mm/s stamping speed (Table 4).

Figure 13 exhibits the obtained stamping parts at the parameters of the two compromise solutions. The forming quality of the obtained stamping parts is good, and no evident defects are observed. However, slight wrinkling is identified in the flange area of the stamping parts under the process parameters of compromise solution 2 because of its large thickening rate. Nevertheless, the slight wrinkling will not affect the final use of the product because the flange area of the obtained parts is cut off in actual production. Therefore, compromise solution 2 is the optimal combination of process parameters from a comprehensive perspective.

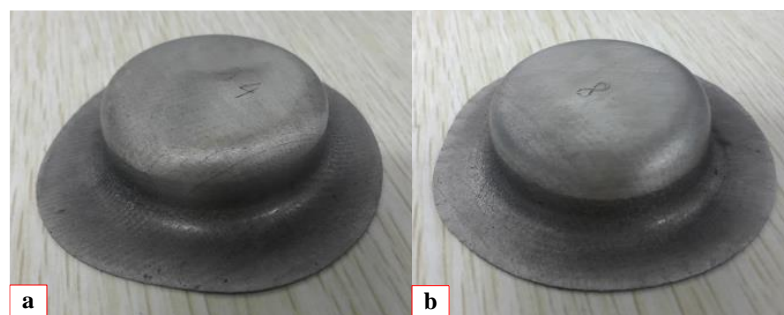


Figure 13. Hot stamping parts of experimentally stamped ZK60 magnesium alloy: (a) Obtained part at the parameters of compromise solutions 1; (b) Obtained part at the parameters of compromise solutions 2.

The thickness variation of a stamping part is an important index of the forming quality. Therefore, the thickness variation of the stamping parts obtained by the hot drawing experiment under the process parameters of compromise solution 2 is compared with that of the simulation results, as shown in Figure 14. The thickness variation distribution of each shell element in the FE model can be read in the postprocessing of the simulation. The thickness variation distribution of the stamping parts is measured along the symmetrical section of the parts by a micrometer. The results show that the thickness variation distribution obtained by the FE method is consistent with that obtained by the experiment, which further verifies the validity and rationality of the FE process simulation of hot stamping.

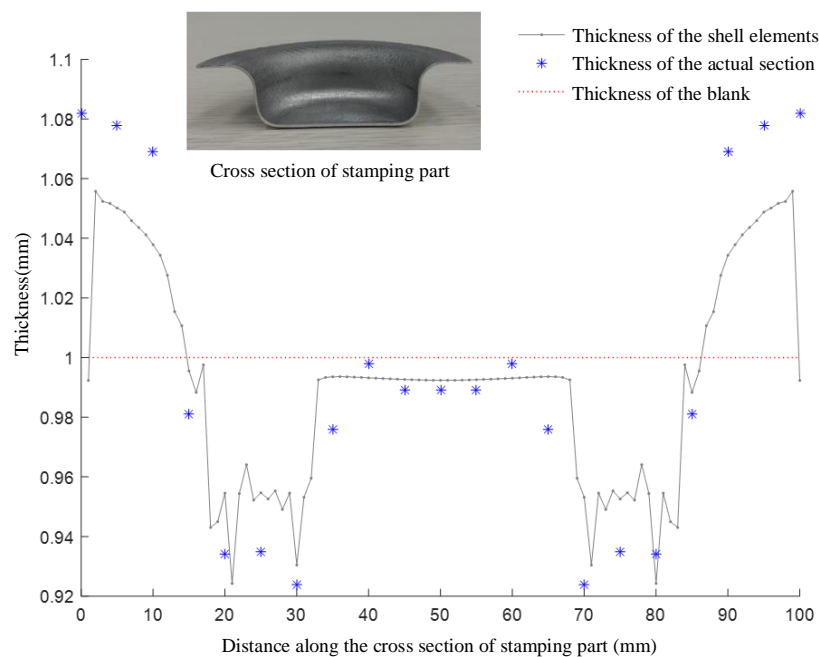


Figure 14. Thickness variation along the symmetrical section of the experimentally obtained parts and simulation result.

6. Conclusions

Hot stamping is developed and widely applied in vehicle production according to the lightweight demands of automobiles. But hot stamping is energy intensive due to the high-temperature forming conditions of blanks. To reduce the energy consumption and improve the energy efficiency of hot stamping, an energy-economizing optimization method for hot stamping is proposed. In this method, the process parameters are optimized to reduce the energy consumption of hot stamping while maintaining the required forming quality.

In this study, the mathematical modelling, simulation, and optimization of ZK60 magnesium alloy sheets hot stamping process were addressed in the aim of improving the energy efficiency and forming quality of the stamping parts. For this purpose, a new multiobjective optimization method is proposed and tested in a real industrial size case study experiment. The model is developed and solved using a multiobjective genetic algorithm (NSGA-II), and offers feasible optimized solutions. The comparison between the numerically-predicted technical parameters of the stamps and the real experimental results demonstrates the applicability of the method. Under the optimized conditions in the case study, a substantial energy consumption reduction, i.e., 17.6%, is shown. This method may serve as a reference for finding proper process parameters to solve the energy inefficiency and high energy consumption problems associated with the metal forming fields.

Author Contributions: Conceptualization, M.G. and L.L.; methodology, M.G.; software, L.L.; validation, M.G., Q.W. and L.L.; formal analysis, Z.M.; investigation, Z.M.; resources, Q.W.; data curation, Z.M.; writing—original draft preparation, M.G.; writing—review and editing, Q.W.; visualization, L.L.; supervision, L.L.; project administration, Q.W.; funding acquisition, M.G. and Q.W. All authors have read and agreed to the published version of the manuscript.

Funding: This research was funded by [key projects of natural science research in colleges and universities of Anhui province China] grant number [KJ2018A0451], [Anhui Major Science and Technology Project] grant number [18030901023], [Suzhou College Scientific Research Foundation Project] grant number [2017JB03], [Suzhou Engineering Research Center for Collaborative Innovation of Mechanical Equipment] grant number [SZ2017ZX07], [Suzhou College Teacher Application Ability Development Workstation] grant number [2018XJYY01], [Opening Project of Suzhou University Research Platform] grant number [2019kyf21, 2019ykf26, 2019ykf27], and [Suzhou College Teacher Application Ability Development Workstation] grant number [2018XJYY01].

Conflicts of Interest: We declare that we have no financial or personal relationships with other people or organizations that can inappropriately influence our work. We confirm that none of the material in the paper, in whole or in part, has been published or is under consideration for publication elsewhere. All the authors listed have approved the manuscript.

References

1. Liu, C.; Zhu, Q.; Wei, F.; Rao, W.; Liu, J.; Hu, J.; Cai, W. An integrated optimization control method for remanufacturing assembly system. *J. Clean. Prod.* **2019**, 119261. [CrossRef]
2. Yang, X. More Efforts are Needed to Promote New Energy. Available online: <https://www.energy.people.com.cn/n1/2019/0307/c71661-30961766.html> (accessed on 21 January 2020).
3. Whalen, S.; Overman, N.; Joshi, V.; Varga, T.; Graff, D.; Lavender, C. Magnesium alloy ZK60 tubing made by Shear Assisted Processing and Extrusion (ShAPE). *Mater. Sci. Eng. A* **2019**, 755, 278–288. [CrossRef]
4. Singh, V.P.; Patel, S.K.; Kumar, N.; Kuriachen, B. Parametric effect on dissimilar friction stir welded steel-magnesium alloys joints: A review. *Sci. Technol. Weld. Join.* **2019**, 24, 653–684. [CrossRef]
5. Karbasian, H.; Tekkaya, A.E. A review on hot stamping. *J. Mater. Process. Technol.* **2010**, 210, 2103–2118. [CrossRef]
6. Gao, M.; He, K.; Li, L.; Wang, Q.; Liu, C. A review on energy consumption, energy efficiency and energy saving of metal forming processes from different hierarchies. *Processes* **2019**, 7, 357. [CrossRef]
7. Bariani, P.F.; Bruschi, S.; Ghiotti, A.; Michieletto, F. Hot stamping of AA5083 aluminium alloy sheets. *CIRP Ann.-Manuf. Technol.* **2013**, 62, 251–254. [CrossRef]
8. Gao, M.; Huang, H.; Wang, Q.; Liu, Z.; Li, X. Energy consumption analysis on sheet metal forming: Focusing on the deep drawing processes. *Int. J. Adv. Manuf. Technol.* **2018**, 96, 3893–3907. [CrossRef]
9. Gao, M.; Liu, Z.; Li, L. Energy consumption analysis focusing on hot stamping of sheet metal. *J. Plast. Eng.* **2017**, 24, 74–81.
10. Shi, C.W.P.; Rugrungruang, F.; Yeo, Z.; Gwee, K.H.K.; Ng, R.; Song, B. Identifying carbon footprint reduction opportunities through energy measurements in sheet metal part manufacturing. In *Glocalized Solutions for Sustainability in Manufacturing*; Springer: Berlin/Heidelberg, Germany, 2011; pp. 389–394.
11. Bosetti, P.; Bruschi, S.; Stoehr, T.; Lechler, J.; Merklein, M. Interlaboratory comparison for heat transfer coefficient identification in hot stamping of high strength steels. *Int. J. Mater. Form.* **2010**, 3, 817–820. [CrossRef]
12. Abdulhay, B.; Bourouga, B.; Dessain, C. Experimental and theoretical study of thermal aspects of the hot stamping process. *Appl. Therm. Eng.* **2011**, 31, 674–685. [CrossRef]
13. Xiao, W.; Wang, B.; Zheng, K. An experimental and numerical investigation on the formability of AA7075 sheet in hot stamping condition. *Int. J. Adv. Manuf. Technol.* **2017**, 92, 3299–3309. [CrossRef]
14. Marler, R.T.; Arora, J.S. The weighted sum method for multi-objective optimization: New insights. *Struct. Multidiscip. Optim.* **2010**, 41, 853–862. [CrossRef]
15. Costa, N.R.; Pereira, Z.L. Multiple response optimization: A global criterion-based method. *J. Chemom.* **2010**, 24, 333–342. [CrossRef]
16. Zhou, J.; Wang, B.; Lin, J.; Fu, L. Optimization of an aluminum alloy anti-collision side beam hot stamping process using a multi-objective genetic algorithm. *Arch. Civ. Mech. Eng.* **2013**, 13, 401–411. [CrossRef]
17. Kitayama, S.; Huang, S.; Yamazaki, K. Optimization of variable blank holder force trajectory for springback reduction via sequential approximate optimization with radial basis function network. *Struct. Multidiscip. Optim.* **2013**, 47, 289–300. [CrossRef]
18. Zhou, J. A Method to Optimize Aluminum Alloy Door Impact Beam Stamping Process Using NSGA-II. *Mater. Sci. Forum* **2013**, 773–774, 89–94. [CrossRef]
19. Xiao, W.; Wang, B.; Zhou, J.; Ma, W.; Yang, L. Optimization of aluminium sheet hot stamping process using a multi-objective stochastic approach. *Eng. Optim.* **2016**, 48, 2173–2189. [CrossRef]
20. Liang, Y. Research and Application on Key Process Experiment of High Strength Steel for Hot Forming. Ph.D. Thesis, Da Lian University of Technology, Dalian, China, 15 December 2013.
21. Gao, M.; Huang, H.; Li, X.; Liu, Z. Carbon emission analysis and reduction for stamping process chain. *Int. J. Adv. Manuf. Technol.* **2017**, 91, 667–678. [CrossRef]

22. Li, L.; Huang, H.; Zhao, F.; Zou, X.; Lu, Q.; Wang, Y.; Liu, Z.; Sutherland, J.W. Variations of Energy Demand With Process Parameters in Cylindrical Drawing of Stainless Steel. *J. Manuf. Sci. Eng.-Trans. ASME* **2019**, *141*, 091002. [\[CrossRef\]](#)
23. Deb, K.; Agrawal, S.; Pratap, A.; Meyarivan, T. *A Fast Elitist Non-dominated Sorting Genetic Algorithm for Multi-objective Optimization: NSGA-II*; Springer: Berlin/Heidelberg, Germany, 2000; pp. 849–858.
24. Zhang, S.; Song, G.; Song, H.; Cheng, M. Deformation Mechanism and Warm Forming Technology for Magnesium Alloys Sheets. *J. Mech. Eng.* **2012**, *48*, 28–34. [\[CrossRef\]](#)
25. Zhang, X.; Cui, Z.; Ruan, X. Warm Forging of Magnesium Alloys: The Formability and Flow Stress of AZ 31B. *J. Shanghai Jiaotong Univ.* **2003**, *37*, 1874–1877.



© 2020 by the authors. Licensee MDPI, Basel, Switzerland. This article is an open access article distributed under the terms and conditions of the Creative Commons Attribution (CC BY) license (<http://creativecommons.org/licenses/by/4.0/>).